

# Slow-Theta-to-Gamma Phase–Amplitude Coupling in Human Hippocampus Supports the Formation of New Episodic Memories

Bradley Lega<sup>1</sup>, John Burke<sup>2</sup>, Joshua Jacobs<sup>3</sup> and Michael J. Kahana<sup>2</sup>

<sup>1</sup>Department of Neurosurgery, Hospital of the University of Pennsylvania, Philadelphia, PA 19104, USA, <sup>2</sup>Department of Psychology, University of Pennsylvania, Philadelphia, PA 19104, USA and <sup>3</sup>School of Biomedical Engineering, Science and Health Systems, Drexel University, Philadelphia, PA 19104, USA

Address correspondence to Dr Bradley Lega, Department of Neurosurgery, The University of Texas Southwestern Medical Center, 5323 Harry Hines Blvd, Dallas, TX 75390, USA. Email: bradley.lega@utsouthwestern.edu

**Phase–amplitude coupling (PAC) has been proposed as a neural mechanism for coordinating information processing across brain regions. Here we sought to characterize PAC in the human hippocampus, and in temporal and frontal cortices, during the formation of new episodic memories. Intracranial recordings taken as 56 neurosurgical patients studied and recalled lists of words revealed significant hippocampal PAC, with slow-theta activity (2.5–5 Hz) modulating gamma band activity (34–130 Hz). Furthermore, a significant number of hippocampal electrodes exhibited greater PAC during successful than unsuccessful encoding, with the gamma activity at these sites coupled to the trough of the slow-theta oscillation. These same conditions facilitate LTP in animal models, providing a possible mechanism of action for this effect in human memory. Uniquely in the hippocampus, phase preference during item encoding exhibited a biphasic pattern. Overall, our findings help translate between the patterns identified during basic memory tasks in animals and those present during complex human memory encoding. We discuss the unique properties of human hippocampal PAC and how our findings relate to influential theories of information processing based on theta–gamma interactions.**

**Keywords:** episodic memory, hippocampus, phase–amplitude coupling, theta

## Introduction

The formation of new memories requires the coordination of neural activity across widespread brain regions. Neural oscillations are thought to play a critical role in this coordination. In support of this hypothesis, it is now established that high-frequency activity in the local field potential is modulated by the phase of low-frequency oscillations. This phenomenon, known as phase–amplitude coupling (PAC), has been well documented in both human and animal studies (Chrobak and Buzsáki 1998; Johnson and Redish 2007; Tort et al. 2007, 2008; Wulff et al. 2009; Cohen et al. 2009; Voytek et al. 2010; Shirvalkar et al. 2010; Maris et al. 2011; Miller et al. 2012; van der Meij et al. 2012; Canolty et al. 2006).

In both humans and animals, the hippocampus is believed to support the formation of new associative or contextually mediated memories. Theta oscillations are thought to impose temporal organization on the coordinated firing of neuronal assemblies, joining changes in membrane depolarization and synaptic connectivity that represent individual memory items with a representation of ongoing time epochs, with context–item associations in humans analogous to item–place associations in animal spatial encoding (Chrobak and Buzsáki 1998; Buzsáki 2005). PAC provides a specific mechanism to join changes in field potential over larger brain areas with activity

of individual neurons and small sets of neuronal assemblies via phase coding (Hasselmo and Eichenbaum 2005; Canolty and Knight 2010). As such, one would expect to see hippocampal PAC during memory encoding and in particular one would hypothesize that hippocampal PAC predicts the quality of such encoding. In rodents, hippocampal PAC has been found to increase during associative learning (Tort et al. 2009). In humans, direct electrophysiological access to the hippocampus is possible in neurosurgical cases, and in a study of working memory (Axmacher et al. 2010) reported that hippocampal PAC during a working memory task increased with memory load. Although working memory is generally thought not to depend on the integrity of the hippocampus, the findings of Axmacher et al. are consistent with recent evidence implicating episodic memory processes in many classic working memory tasks (Olson et al. 2006). Although hippocampal signals cannot be resolved using noninvasive recordings, a recent magnetoencephalography study has suggested that memory-related increases in PAC may be generated by sources in the mesial temporal lobe (Staudigl and Hanslmayr 2013). Direct hippocampal recordings in humans could be used to modify the influential theories of theta–gamma interaction during item encoding that have been developed using animal data (Hasselmo and Eichenbaum 2005). New information about the pattern of phase preference for gamma coupling in the mesial temporal structures may motivate modifications specific to human data.

Here we sought to establish whether there is a unique signature of hippocampal PAC during memory encoding. To do this we analyzed recordings from 56 neurosurgical patients who had both hippocampal depth-electrodes and neocortical recordings from subdural grids and strips. These data allowed us to directly test whether hippocampal and neocortical PAC reflect common or distinct neural phenomena, and to establish the properties of hippocampal PAC during episodic memory encoding. The attributes we uncovered for hippocampal PAC are consistent with animal data but also include novel patterns of phase coupling and frequency preference that are unique to human data.

## Experimental Procedures

### Participants and Electrodes

Fifty-six participants with medically refractory epilepsy underwent implantation of standard platinum–iridium recording electrodes, consisting of surface electrodes (4-mm disks) and depth electrodes placed in subcortical structures (2-mm cylindrical contacts). Placement was guided by clinical concerns for seizure localization. Localization of electrodes in the brain was

achieved by co-registering postop computed tomography scans with magnetic resonance images using FSL software. These were mapped to Montreal Neurological Institute and Talairach coordinates. Members of the clinical team verified the intrahippocampal location of depth electrodes at the time of placement. In addition, a manual review of electrode location for 231 of the depth electrodes was undertaken by clinically trained personnel prior to this analysis by re-examining the radiographic images to identify subtle differences in mesial temporal location (i.e., hippocampus vs. uncus, etc.). Location of the surface electrodes was determined using Talairach coordinates. Temporal lobe electrodes in Brodmann's areas 21 and 22 and frontal contacts in areas 6, 8, 9, 10, and 46 were included in the analysis. Electrodes corresponding to site of ictal onset were excluded. In total, our dataset included 1145 electrodes (336 hippocampal, 802 temporal lobe, and 322 frontal lobe electrodes). A subset of this data (33 of 56 participants) comprised the set for our previous publication about theta oscillations in the hippocampus (Lega et al. 2011). Side of language dominance was recorded for participants in whom clinical concerns dictated the need for preoperative Wada or functional magnetic resonance confirmation of the hemisphere of language dominance.

### IRB Review

All participants in this investigation underwent informed consent under a series of IRB reviews at all institutions from which the participants were drawn. Research was conducted in accordance with the principles of the Declaration of Helsinki.

### Data Processing

Recordings were initially sampled between 256 and 2000 Hz, depending upon the equipment and preferences of the clinical personnel at each institution. Five patients were included for which the analysis was limited to the low gamma band only due to sampling rate. For analysis, the raw data were resampled at 500 or 125 Hz (the latter for the 5 patients mentioned above) and a Butterworth filter 2 Hz in width was applied at either 50 or 60 Hz to eliminate line noise. A kurtosis method for artifact rejection (threshold of 4) was applied as previously described (Sederberg et al. 2003). The downsampled electrocorticography (ECoG) signal was initially analyzed using Morlet wavelets (Addison 2002). Logarithmically spaced wavelets between 2 and 128 Hz were convolved with the ECoG signal spanning 1400 ms (between 400 and 1800 ms following the onset of a memory encoding item). We excluded the initial 400 ms following stimulus onset to avoid confounding effects of evoked components immediately following stimulus onset. While some evoked changes can occur past this 400-ms period, we believed that excluding this initial portion would improve the signal-to-noise ratio for the quantification of PAC. Results using a longer time window are included in the Supplementary Material. A 1000-ms buffer was used on both sides of this 1400-ms time window of data. We extracted the instantaneous power and phase across the entire ECoG frequency spectrum using wavelets for the initial analysis (Fig. 2) in order to avoid making a priori assumptions about the identity of frequency bands participating in PAC. For the subsequent analyses in which we sought to compare among predefined frequency bands, we used the Hilbert transform to extract phase and

power information for the slow-theta (2.5–5 Hz), theta (4–9 Hz), alpha (9–16 Hz), beta (16–24 Hz), low gamma (30–70 Hz), and high gamma (70–128 Hz) frequency bands over the same segment of ECoG data. The ranges for these frequency bands were determined in part by our own previous findings and other recent publications that posit a memory-relevant functional role for oscillations in the sub-5 Hz frequency range (Cornwell et al. 2008; Chen et al. 2013; Watrous, Lee et al. 2013; Watrous, Tandon et al. 2013). We used this information when categorizing activity in the 2.5–5 Hz range as “slow-theta.” We defined the edges of the 4–9 Hz theta band to capture the full frequency range for traditional theta activity; for the alpha and beta bands we used an extended range of 9–16 and 16–24 Hz to include a nonoverlapping section of activity outside of the main frequency bands of interest (slow-theta and normal theta) below the gamma bands. We acknowledge that our results in these frequency ranges may show slightly different properties with more narrow bands, but our unbiased compilation of activity across the spectrum (see Results, first section) suggested stronger effects occur primarily for theta and slow-theta coupling.

### Phase–Amplitude Coupling

For the identification of significant PAC following item encoding, we first filtered and downsampled the raw ECoG signal (see above) to obtain the ECoG time series around each encoding event,  $x_E$ . We then obtained the instantaneous power and phase representations of the  $x_E$  at each logarithmically defined center frequency and a priori defined frequency band using the Morlet convolution and Hilbert transform, respectively. The wavelet approach allowed us to characterize PAC with high spectral resolution in an unbiased manner, whereas the Hilbert approach facilitated the comparison of PAC across electrodes at particular frequency bands while limiting the number of comparisons to the frequency bands of interest defined a priori. In both cases, we examined all pair-wise frequency combinations for PAC. Specifically, the phase of the lower frequency in the pair ( $\phi_{f_1}$ ; the “phase-modulating frequency”) and the amplitude of the higher frequency in the pair ( $A_{f_2}$ ; the “amplitude-modulated frequency”) were used to identify PAC (Tort et al. 2010). We identified PAC by binning the power values of each  $A_{f_2}$  according to the phase of the oscillation at each  $\phi_{f_1}$  (10 phase bins) for each time sample within the 1400-ms time window used for analysis. We then performed an ANOVA on the phase-binned power values with the phase bin held as a fixed effect, allowing us to identify a single  $P$  value for PAC. Significant instances of PAC were determined using a permutation procedure, described below. Using 10 phase bins reduces the computational load of the analysis, which can become onerous when incorporating a shuffle procedure to identify significant PAC.

For electrodes that exhibited significant PAC using this ANOVA framework, we next tested whether, across all electrodes, PAC occurred at a consistent phase of  $\phi_{f_1}$ . To accomplish this, we first identified electrodes that exhibited significant PAC for a given  $A_{f_2}$ ,  $\phi_{f_1}$  combination. We next used the real and imaginary components of  $\phi_{f_1}$  as independent variables in a regression equation with  $A_{f_2}$  as the dependent variable (Penny et al. 2008; Vinck et al. 2010). We converted the resulting regression coefficients to radians (using the 4 quadrant  $\tan^{-1}$  transform) to obtain a representation, across time, of a

single phase value that best predicted power at higher frequencies within each electrode across all encoding events. Circular regression takes account of the separate linear and circular properties of amplitude and phase, as has been described previously (Vinck et al. 2010). This was done initially using the wavelet-extracted power and phase information (see Fig. 2, bottom row), and then for the entire frequency band using the Hilbert method. The most predictive phase value was obtained within each electrode. We next compiled the resulting phase values into a vector and tested for nonuniformity of the phase distribution using the Rayleigh test applied across all electrodes that exhibited significant PAC in each frequency band. We compared phase distributions directly between frequency bands by applying a nonparametric test for circular distributions as described by Fisher (1993).

Finally, we sought to identify electrodes that exhibited significant differences in PAC between successful and unsuccessful encoding. Here, successful encoding was operationalized using the subsequent memory (SM) paradigm (Paller and Wagner 2002). Specifically, words that were presented during the encoding period and successfully retrieved during the recall period are considered successfully encoded (e.g., the words CAR, FENCE, and PEN in Fig. 1A). Likewise, words that were not retrieved during the recall period are considered unsuccessfully encoded (e.g., the words FLAME and PASTE in Fig. 1A). Using PAC in the SM paradigm required a trial-by-trial measure of PAC, which we obtained via the modulation index (MI) using 10 phase bins. While the ANOVA method is a robust way to identify significant PAC, using the MI is necessary for a within-electrode comparison of PAC on a trial-by-trial basis.

The normalized, average power in each phase bin (for each trial) was compared with a uniform distribution using the Kullback-Leibler (KL) distance to obtain the MI, as described in previous reports (Tort et al. 2009, 2010; Canolty and Knight 2010). The MI varies between 0 and 1, where 0 represents a uniform distribution across phase bin, and 1 represents a delta-like concentration of power at one particular phase bin.

### Statistical Procedure

To test for the statistical reliability of PAC, we used a permutation procedure. For the identification of PAC at frequency–frequency pairs using the ANOVA model described above (for both the wavelet and Hilbert approaches), we first converted the  $P$  value from the ANOVA to a  $z$  value using the inverse normal transformation.  $z$  values were obtained for each  $A_{f_2}$  and  $\phi_{f_1}$  pair for each electrode in our dataset. We then compared the actual  $z$  values to an empirically derived null distribution of  $z$  values obtained by randomly shuffling the phase label for the binned power values in the ANOVA model (500 shuffles). Significant PAC for each electrode within each pixel was then determined by comparing the  $z$  value from the real data to the distribution of  $z$  values from the shuffled data.  $z$  values more extreme than the smallest 5% from the shuffled distribution were considered significant. The shuffle procedure allowed us to generate an unbiased estimate of the Type I error rate. The pattern of PAC across the spectrum was examined by compiling the number of electrodes that exhibited significant PAC within each  $A_{f_2}$  and  $\phi_{f_1}$  pair into a summary histogram. We utilized this shuffle procedure given the likely nonindependence of each trial comprising the PAC measurement.

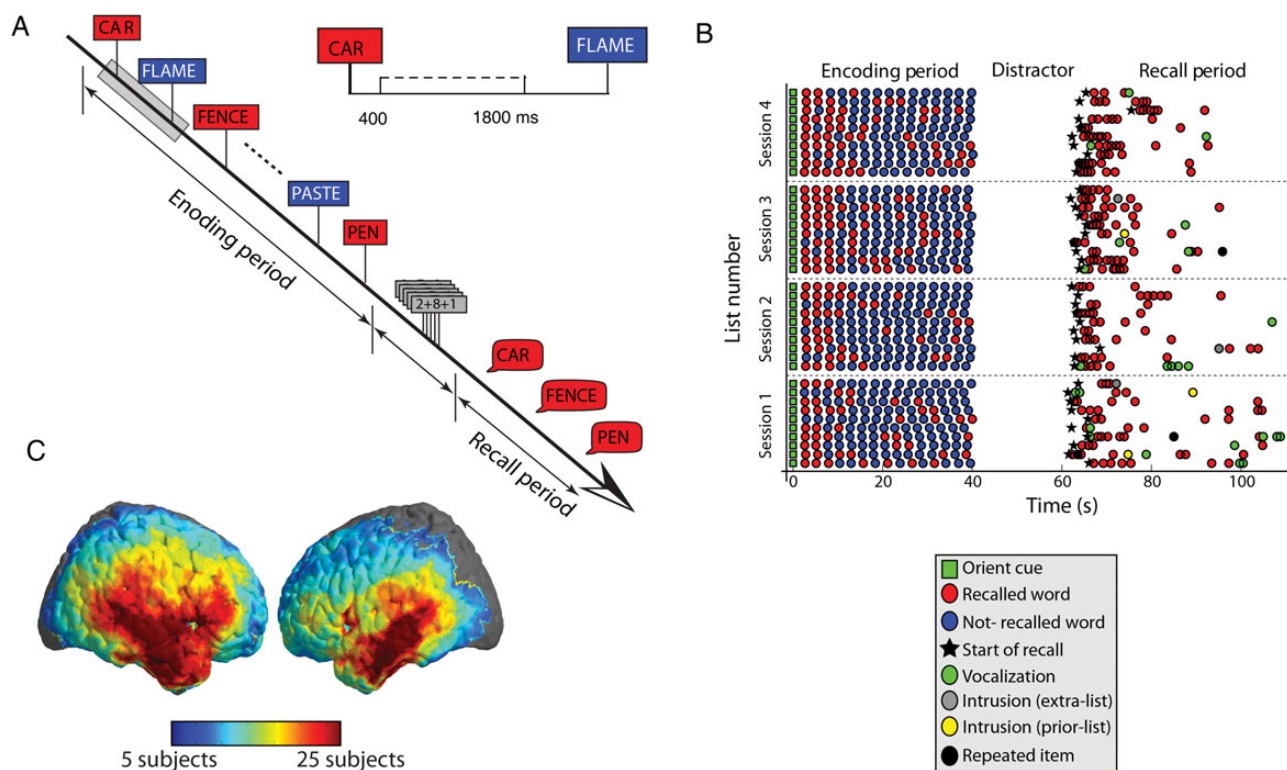


**Figure 1.** Summary of the Free Recall task and the distribution of cortical electrodes in our dataset. (A) Timeline of a single trial in Free Recall task. The time bin from 400 ms following the onset of the memory item through 1800 ms was used for analysis. (B) Example of all trials completed by a single participant across 4 sessions. The serial position of correct recall items is shown, along with the timing of item retrieval following the onset of the recall cue. (C) Brain plot showing the number of participants with electrodes located in each portion of the neocortex. All 56 participants included in the analysis had at least 1 hippocampal electrode.

To test for differences in PAC across frequency bands and anatomical regions, we extracted a single value for phase and power at each time sample using the Hilbert transform applied to the frequency bands as described above. For each electrode, we were then able to extract a test statistic for PAC (the effect size from the ANOVA, or  $\eta^2$  value) for every frequency band (slow theta, 4–9 Hz theta, alpha, and beta, separately for high and low gamma modulation). These test statistics were compiled into a vector consisting of a single value for each non-gamma frequency band for each electrode separately for low and high gamma band modulation (number of elements in vector equivalent to number of electrodes at each location). We tested for differences in the pattern of PAC between hippocampus and temporal and frontal cortex by applying an ANOVA to these distributions for the slow-theta and theta bands, with frequency band held as a fixed effect and location as a random effect. For this analysis, we used an FDR correction procedure to account for the comparisons for 2 frequency bands (low and high gamma or 4–9 Hz vs. slow-theta) across the 3 brain locations. Given that this test was across test statistics from different electrodes, we used the parametric ANOVA without an additional shuffle procedure.

In contrast, we used a nonparametric Mann–Whitney *U*-test to compare PAC during successful versus unsuccessful item encoding because of the need to compare distributions of MI values rather than test statistics extracted for each electrode. We identified significant differences in PAC by shuffling values for successful and unsuccessful encoding trials 500 times and determining the position of *W* within the distribution of shuffled *W*'s. We quantified the number of electrodes that exhibited significant differences in PAC in either direction (greater for unsuccessful vs. greater for successful encoding) and identified frequency bands (for modulating phase) for which the number of electrodes exceeded the 5% error rate expected by chance. We classified electrodes as “PAC+” if they exhibited significantly greater PAC during successful item encoding, and “PAC–” if they exhibited significantly greater PAC during unsuccessful encoding.

To test for a relation between preferred phase and successful encoding, we first extracted the preferred phase for PAC (as described above) for electrodes that were identified as exhibiting significant differences between successful and unsuccessful encoding via the permutation test of the MI distributions. Then, we used a  $\chi^2$  test to examine whether the differences in the proportion of electrodes that exhibited significant PAC was different among the frequency bands, using direct comparisons for slow-theta versus 4–9 Hz theta bands. Finally, we directly compared PAC effects to subsequent memory effects (SMEs). To do this, we extracted a single test statistic at each electrode comparing gamma band power during successful and unsuccessful encoding, using a two-sample *t*-test (Burke et al. 2013). We then correlated this SME *t* statistic with the *z* value extracted from the nonparametric test comparing MI during successful and unsuccessful encoding, using Pearson's coefficient to test for significant correlation. We performed this analysis separately for SME in the high gamma, low gamma, and slow-theta bands in the hippocampus, as suggested by our previous data (Lega et al. 2011).

## Results

We analyzed intracranial EEG recordings from 56 participants undergoing invasive evaluation during a phase II clinical

investigation to identify an epileptic focus for possible resective surgery. Data were from a subgroup of the patients studied at 4 institutions over a period of 13 years with the subgroup defined as patients who had well-localized depth electrodes in the hippocampal formation. Recordings were from a total of 336 hippocampal electrodes, 802 temporal lobe electrodes, and 322 frontal lobe electrodes. Participants studied lists of 15–20 common nouns presented one at a time. After a brief arithmetic distractor task participants were given 45 s to recall all the words they could remember in any order (Fig. 1A; see Materials and Methods). Participants recalled an average of 23.6% of study items and made an average of 4.4% incorrect recalls (these intrusion errors were not a focus of the present analysis).

### Hippocampal and Neocortical PAC Exhibit Different Properties

We first asked whether and at what frequencies recordings from each electrode exhibited significant PAC during memory encoding. By binning the power information according to the phase of the lower frequency oscillations, we identified significant PAC at every frequency (for modulating phase,  $\phi_{f_1}$ )–frequency (for modulated amplitude,  $A_{f_2}$ ) step in the frequency domain. Step size was logarithmically spaced from 2 to 64 Hz for phase and 2 to 128 Hz for amplitude. An example of this analysis is presented for 3 electrodes from the dataset in Figure 2A. In the figure, normalized power at the higher frequency (modulated amplitude) is averaged across all word presentation events according to the phase of the lower frequency oscillation (modulated phase). The examples show instances in which the power of the high-frequency oscillation critically depends on the phase of the lower-frequency oscillation. This is consistent with a number of recent publications that show PAC is a ubiquitous finding in human intracranial recordings (Canolty et al. 2006; Canolty and Knight 2010; van der Meij et al. 2012). To test for significant phase modulation of amplitude, we used a 1-way ANOVA with an associated shuffle procedure (see Materials and Methods for details) to derive a *P* value at each  $\phi_{f_1} - A_{f_2}$  step across the spectrum for each electrode in the dataset. An example of the distribution of *P* values for 3 individual electrodes is given in Figure 2B. The exact  $\phi_{f_1} - A_{f_2}$  steps exhibiting significant PAC were different among different electrodes, as the figure illustrates. We next extracted a single preferred phase value for PAC at each electrode for each of those frequency–frequency pairs that exhibited significant PAC and plotted the resultant phase values in frequency–frequency space. The example electrodes in Figure 2C are illustrative: the preferred phase may differ among electrodes, though within a single electrode the phase value is highly conserved across frequency space.

We next asked if the pattern of PAC in frequency–frequency space differed across hippocampal, temporal and frontal cortices. We compiled the number of significant electrodes at each frequency–frequency step into a histogram separately for the 3 anatomical areas of interest (Fig. 3A). We found that hippocampal electrodes exhibited a maximal PAC with modulating phase frequencies in the slow-theta band: Coupling is strongest between the phase of slow-theta oscillations (in the 2.5–5 Hz range) and the power of both low (35–70 Hz) and high (70–130 Hz) gamma oscillations. Consistent with existing data, coupling also occurs at frequency–frequency pairs across the spectrum, including within the traditional 4–9 Hz theta band

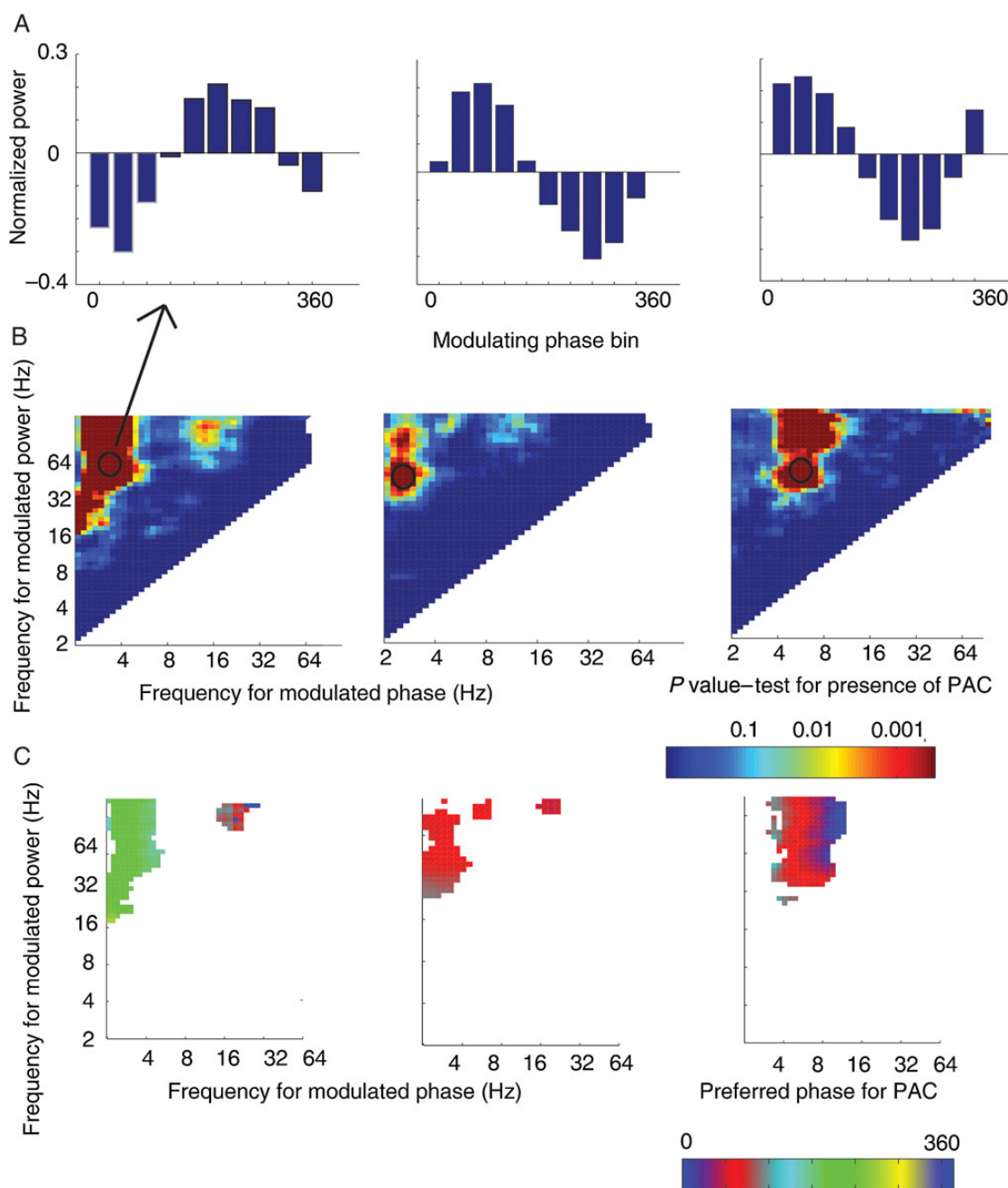


**Figure 2.** Identification of phase–amplitude coupling (PAC). (A) Mean normalized power values across 10 phase bins for a single frequency (modulating phase)–frequency (modulated amplitude) step. This same analysis was performed at each step in the spectrum. (B) Summary graph for all frequency–frequency steps showing the  $P$ -value at each step from the permutation procedure detecting significant PAC. Left and center plots show a concentration of effect in the slow-theta band (for gamma modulation) while the plot in right-hand column shows 4–9 Hz theta modulation of gamma band power. Circle indicates the  $\phi_{f_1} - A_{f_2}$  pair from which the binned power values (shown in the top row) were drawn. (C) Preferred phase for PAC as determined by circular regression. Phase values for frequency–frequency pairs with significant PAC are plotted. Preferred phase is conserved across significant pairs within the frequency band.

(van der Meij et al. 2012), but the effect appears strongest in the slow-theta range (for modulating phase) in the hippocampus. 45 of 56 participants ( $P < 0.0001$ , binomial test) had at least one electrode in the hippocampus that exhibited significant PAC for modulation of high and low gamma by slow-theta phase.

The electrodes in the lateral temporal (Brodmann areas 21 and 22) and frontal sites (Brodmann areas 6, 8, 9, 10, and 46) displayed a different pattern of PAC during encoding when compared with electrodes in the hippocampus. Specifically,

the preferred phase-providing frequency for gamma band modulation is concentrated in the 4–9 Hz theta band in the cortex, with the low gamma band exhibiting greater modulation than the high gamma band in both of these locations when compared with the hippocampus (Fig. 3A, columns 2 and 3). The observation of a differential theta frequency preference between the hippocampus and neocortex links our findings with a growing body of research suggesting that functional human hippocampal theta oscillations occur at lower

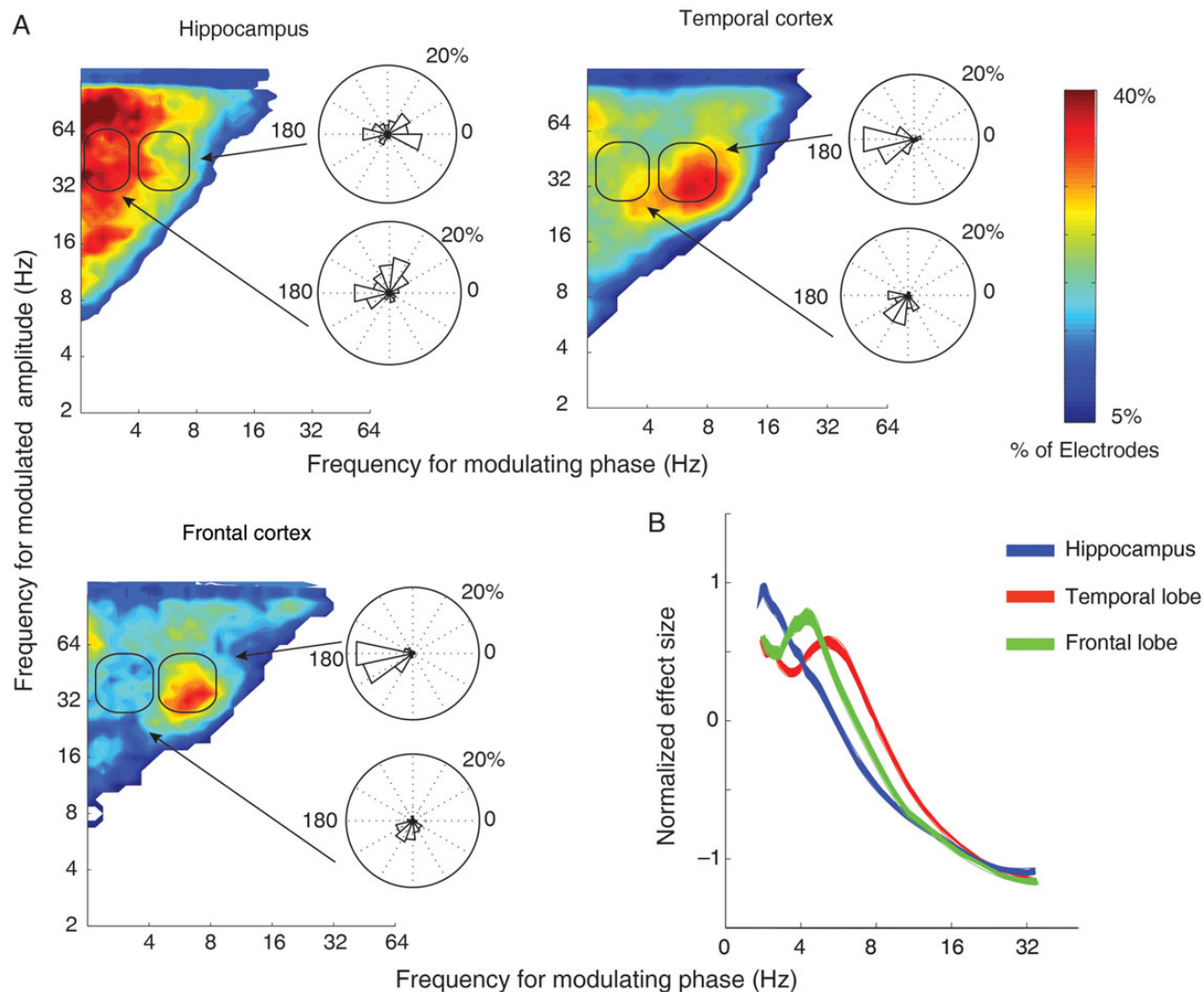


**Figure 3.** Phase–amplitude coupling aggregated across all recordings. (A) Histograms compiling total number of electrodes exhibiting significant PAC in each brain location during item encoding. For the hippocampus, high and low gamma amplitude is most strongly modulated by slow-theta phase while, in the temporal and frontal cortex, low gamma amplitude is preferentially modulated by 4–9 Hz theta phase. Color scale is a percentage of all electrodes in each brain area exhibiting significant PAC. Inset roseplots are histograms compiling the preferred phase for low gamma band modulation by slow-theta (bottom) and 4–9 Hz theta (top) phase as a percentage of all the electrodes in each brain area. For hippocampal slow theta, preferred phase exhibits a bimodal pattern with a concentration at  $\sim 70^\circ$  and again at  $\sim 180^\circ$ . Four- to nine-Hertz theta phase in the temporal and frontal cortex is strongly clustered at  $180^\circ$ . (B) Normalized effect size at each frequency for gamma band PAC. The effect for the hippocampus is highest in slow-theta, temporal/frontal cortex in 4–9 Hz theta range.

frequencies ( $<5$  Hz) than analogous theta activity in the rat (Lega et al. 2011; Watrous, Lee et al. 2013).

To formally test for the interaction between anatomical location and the preferred frequencies for PAC, we used the effect size ( $\eta^2$  value) drawn from the ANOVA applied to 10 bins of gamma band power (low and high gamma tested separately), binned according to the phase of the 2.5–5 Hz and 4–9 Hz bands. We then extracted the effect size for each electrode in the data set. We used the effect size values to create separate vectors describing slow-theta and 4–9 Hz theta modulation of gamma band amplitude in both anatomical locations (4 vectors of effect size values). We tested for a difference in the strength of gamma modulation by slow theta versus 4–9 Hz theta between anatomical locations using an interaction model with location as a random effect. The difference in PAC for modulation of low gamma band power between the temporal cortex and hippocampus was highly significant ( $F = 21.01$ ,  $P < 0.001$ ). The difference in pattern was also significant between the

hippocampus and the frontal cortex ( $F = 24.08$ ,  $P < 0.001$ ). For a subject-level analysis, in which information across all electrodes was collapsed by subject, the difference was also significant for the temporal cortex ( $F = 3.71$ ,  $P = 0.048$ ) though not the frontal cortex ( $F = 3.22$ ,  $P = 0.091$ ). The effect was not significant for differences in HG PAC in the temporal cortex ( $F = 1.47$ ,  $P = 0.45$ ), owing to a more even distribution of high gamma modulation by both slow theta and 4–9 Hz theta in the cortical locations (larger slow-theta effect in the cortex for HG). For the frontal cortex, the difference remained significant:  $F = 5.94$ ,  $P = 0.011$ . The results of this interaction model confirm the apparent pattern we observed in the summary histograms describing PAC in frequency–frequency space (Fig. 3): hippocampal PAC is strongest for slow-theta phase modulation of the gamma band, while in the neocortex 4–9 Hz theta phase modulates gamma amplitude. Figure 3B shows a plot of normalized effect size at each phase-modulating frequency for all 3 brain locations. The relative PAC magnitude in the hippocampus

is highest for slow-theta frequencies when compared with the other locations across all electrodes in the dataset. This analysis of PAC during memory encoding contributes to the idea that hippocampal and neocortical theta oscillations represent distinct neural phenomena, and the PAC difference between the hippocampus and neocortex implies that PAC serves a unique functional role in memory formation given the different functional properties of these brain regions.

### **Changes in PAC Predict Successful Item Encoding**

We next asked whether the magnitude of PAC during encoding predicts subsequent recall. Previous studies comparing trial-by-trial spectral activity during the encoding of episodic memory items have shown that while theta power strongly predicts memory encoding, the direction of this effect is highly variable, frequently exhibiting opposite effects across recordings from a given brain region in a given participant (Sederberg et al. 2007; Lega et al. 2011). Using a trial-by-trial measure of PAC, termed the MI (see Materials and Methods), we found that PAC also exhibits a heterogeneous pattern of increases and decreases associated with successful memory encoding. Electrodes that exhibited a decreased MI during successful encoding were labeled PAC<sup>-</sup>, and those that exhibited an increase in PAC were labeled as PAC<sup>+</sup>. We compared these effects for slow-theta and 4–9 Hz theta oscillations between hippocampus and neocortex.

In the hippocampus, the slow-theta band but not the 4–9 Hz theta band exhibited a significant number of PAC<sup>+</sup> electrodes (higher PAC during successful item encoding; 10.1% of electrodes,  $P < 0.001$ , binomial test). Both frequency bands exhibited a significant number of PAC<sup>-</sup> electrodes (15.1% and 13.1%, respectively). The fraction of electrodes that exhibited either PAC<sup>+</sup> or PAC<sup>-</sup> effects was greater for the slow-theta band than for the 4–9 Hz theta band in the hippocampus, though it did not survive correction and was not significant ( $\chi^2 = 3.80$ ,  $P = 0.083$ ). In the temporal cortex, the effect was less specific. A reliable number of PAC<sup>+</sup> electrodes were found only for the 4–9 Hz theta band, and both slow theta and 4–9 Hz theta exhibited a significant number of PAC<sup>-</sup> electrodes. The difference in counts was not different between the frequency bands, however ( $\chi^2 = 0.321$ ,  $P = 0.650$ ; Fig. 4A). In the frontal cortex, reliable numbers of electrodes in the 4–9 Hz band but not the slow-theta band exhibited significant PAC<sup>+</sup> and PAC<sup>-</sup> effects. The difference in counts between slow-theta and 4–9 Hz theta was not significant, though the 4–9 Hz proportion was higher ( $\chi^2 = 3.13$ ,  $P = 0.130$ ). This pattern of PAC differences during item encoding matches that which we have observed for SMEs, in which the hippocampus exhibits a relatively greater positive effect in the slow-theta band while a more nonspecific negative effect occurs simultaneously (Lega et al. 2011; Burke et al. 2013). That is, while there is a general subgamma decrease in activity during successful item encoding, the hippocampus exhibits a unique positive effect in the slow-theta band.

### **Increased Hippocampal PAC Occurs When Gamma Oscillations Are Coupled to the Trough of the Slow-Theta Oscillation**

Animal recordings and computational models suggest that the specific phase of theta–gamma coupling affects learning based on coincident membrane activation and associated LTP (O’Keefe and Recce 1993; Hasselmo and Eichenbaum 2005;

Douchamps et al. 2013). To test this hypothesis in our human recordings, we separately computed PAC for slow-theta and 4–9 Hz theta as the phase-modulating frequency, and for low gamma and high gamma as the modulated amplitude. We then used circular regression to identify the preferred phase across 10 phase bins (see Materials and Methods). In the hippocampus, the phase preference for slow-theta PAC showed a bimodal distribution, with a group of electrodes exhibiting a preferred PAC phase of 180° and another of ~70° (Fig. 3A, inset). For 4–9 Hz theta, the distribution was concentrated at 180° and near 0° in the hippocampus. These distributions were significantly different (mean for slow theta = 119, 4–9 Hz = 54°,  $P = 0.023$ ). In the temporal cortex, the bimodal distribution for phase preference was absent for both frequency bands (Fig. 3A, inset, columns 2 and 3). Slow theta exhibited a phase preference concentrated at 250°, while for 4–9 Hz theta the distribution was centered at 180°. These 2 distributions (comparing slow theta to 4–9 Hz theta in the temporal cortex) were significantly different (circular mean = 248 vs. 194°,  $P < 0.001$ ). We then tested the distributions for slow theta and 4–9 Hz theta directly between the hippocampus and temporal cortex. For both, the differences were highly significant ( $P < 0.001$ ). The phase distributions in the frontal cortex were nearly identical to those in the temporal cortex, with a mean phase for slow theta of 247° and for 4–9 Hz theta of 191°.

We sought to further explicate the bimodal distribution of the preferred phase for modulation that we identified in the hippocampus. We did this by examining separately the phase distributions for PAC<sup>+</sup> and PAC<sup>-</sup> electrodes, restricting the comparison of distributions of phase preference values only to those electrodes that exhibited a significant difference in PAC magnitude (as measured by the MI via a subsequent memory paradigm) during successful encoding. We created 2 vectors of phase values according to whether PAC increased or decreased during successful encoding (PAC<sup>+</sup> and PAC<sup>-</sup>). The bimodal distribution of phase preference for hippocampal slow theta appears to be a result of different phase preferences for PAC<sup>+</sup> and PAC<sup>-</sup> electrodes. The phase preference for PAC<sup>+</sup> electrodes is concentrated more strongly near ~180°, while for PAC<sup>-</sup> electrodes it is centered at ~70° (Fig. 4B). This difference in phase distributions was significant (mean = 72 vs. 149°,  $P = 0.007$ ). A matching pattern was not identified for 4–9 Hz theta phase preference values, in which the distributions were not different between PAC<sup>+</sup> and PAC<sup>-</sup> electrodes (mean = 282 vs. 298°,  $P = 0.870$ ). In the temporal and frontal cortex, no difference in phase preference was noted between PAC<sup>+</sup> and PAC<sup>-</sup> electrodes in either the slow-theta band or the 4–9 Hz theta band ( $P > 0.20$  for all comparisons).

### **Comparison of PAC with Power Differences (SME)**

For our final analysis, we sought to address the relationship between PAC and the gamma and slow-theta band SMEs that we have previously described using intracranial data (Sederberg et al. 2003; Lega et al. 2011). To accomplish this, we looked for the correlation between the  $z$  value comparing PAC during successful and unsuccessful item encoding and the  $t$  statistic testing differences in power (magnitude of the SME) during encoding. For the gamma band SME, there was no significant correlation in either the positive or negative direction with the magnitude of the PAC effect ( $\rho = 0.041$ ,  $P = 0.49$ ). The lack of correlation between PAC and the gamma SME suggest

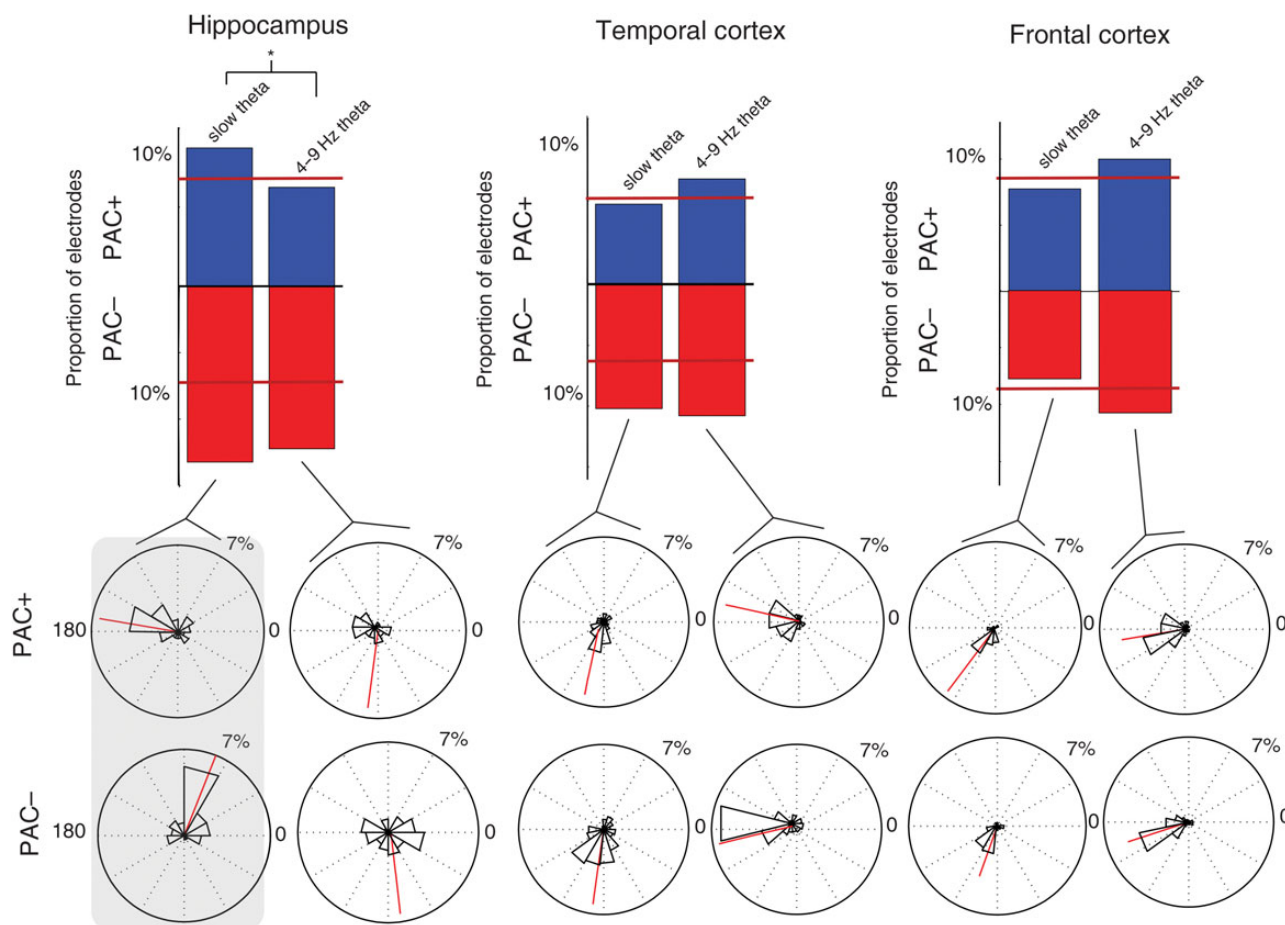


**Figure 4.** Comparison of PAC during successful and unsuccessful item encoding. (A) Histograms showing number of electrodes that exhibit a significant difference in magnitude of PAC (for gamma band coupling) for the slow-theta and 4–9 Hz theta bands. Percentage refers to fraction of electrodes from within each of 3 brain regions. Red segment at bottom indicates PAC– electrodes (greater PAC during unsuccessful encoding) and blue segment indicates PAC+. For hippocampus, asterisk indicates that counts for slow-theta band were significantly greater than for 4–9 Hz band. Red lines across the bars indicate the number of electrodes of the type I error rate. (B) Histogram compiling the preferred phase for PAC for the electrodes included in the histograms above (PAC+ and –). Red line indicates the mean phase value for the entire distribution. Highlighted box on left indicates group for which a significant difference in the distribution of phase values exists between PAC+ and PAC– electrodes (hippocampal slow-theta band) with PAC+ electrodes exhibiting a phase preference clustered at the trough of the oscillation.

that the presence of gamma SME effects during encoding are not confounding the measurement of theta–gamma PAC [this theoretical problem has been described, though not observed, in human PAC (Axmacher et al. 2010)]. For the slow-theta band, we observed a significant positive correlation between the SME and magnitude of the PAC effects ( $\rho = 0.299$ ,  $P < 0.001$ , Fig. 5). This positive correlation makes intuitive sense: as slow-theta power increases (akin to rodent theta), the higher amplitude slow-theta oscillations entrain gamma band activity with more efficiency resulting in greater theta–gamma PAC. When slow-theta power is low, PAC is weak.

## Discussion

In this study, we sought to apply the analysis of PAC to human cortical and hippocampal activity during memory encoding. Our results represent the first examination of human intracranial recordings for evidence of PAC during episodic memory formation. They build upon previous efforts in the human and animal literature to elucidate the role of PAC to characterize the brain networks involved in the encoding of novel memory

items. Our chief findings in this regard are: 1) PAC occurs at a diversity of frequencies, but in the hippocampus it is strongest in the 2.5–5 Hz slow-theta band while in the neocortex it is strongest in the 4–9 Hz theta band. The phase preference for PAC is different for the slow-theta band when compared with 4–9 Hz theta bands both in the hippocampus and the neocortex; 2) A subset of electrodes in the hippocampus exhibits increased PAC during successful encoding, while a different subset exhibits increased PAC during unsuccessful encoding (PAC+ and PAC– electrodes); 3) In the hippocampus, the preferred phase for these 2 subsets of electrodes is different. PAC+ electrodes exhibit a preferred phase near the trough of the ongoing slow-theta oscillation; 4) Increases in slow-theta PAC were associated with increased slow-theta oscillatory power during successful encoding.

Our findings point to the slow-theta band as the principal source for the modulating phase of PAC in the hippocampus. The possibility of memory-relevant oscillatory activity in the slow-theta frequency range has gained traction in the last 3 years as numerous investigations using intracranial recordings have pointed to activity within this band during memory processes (Jacobs 2014). We use the term “slow-theta” to help

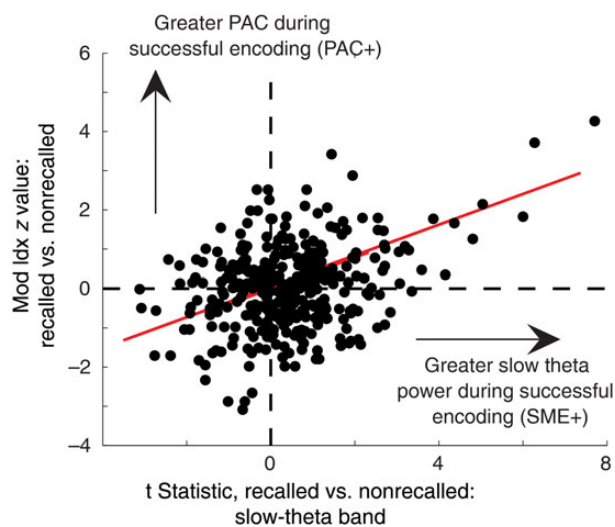


**Figure 5.** Relationship between hippocampal SME and PAC effects. Scatterplot of *t* statistic comparing slow-theta band power during successful and unsuccessful item encoding versus *z* value for PAC during item encoding across all hippocampal electrodes in the dataset. Plot illustrates a highly significant positive correlation between slow-theta SME and PAC differences during encoding. This indicates that as slow-theta power increases at a given electrode, the slow-theta oscillation more efficiently entrains gamma oscillations during successful encoding.

convey the functional properties of this oscillation and because the range of the oscillation, according to our previous analysis, extends beyond the traditional 4-Hz cutoff of the delta band (Lega et al. 2011). Specifically, data analyzing hippocampal slow oscillatory activity during REM sleep implicate sub-4 Hz oscillations in gamma band modulation and entorhinal-hippocampal synchrony (Clemens et al. 2009), while human iEEG recordings during working memory, autobiographical memory, and spatial navigation include evidence of functionally relevant oscillatory activity in this frequency range (Rutishauser et al. 2010; Axmacher et al. 2010; Steinvorth et al. 2009; Fell et al. 2011; Watrous, Lee et al. 2013). Data from Axmacher et al. (2010) demonstrate an increase in PAC in the 4–9 Hz theta range during a working memory task although sub-5 Hz effects were also present. In our data, significant PAC effects were present in the 4–9 Hz frequency band, but the hippocampal slow-theta band contributed the largest fraction of electrodes exhibiting PAC (see Fig. 2, third column). This mild disparity may reflect differences in underlying networks for working versus episodic memory encoding (Tulving 1983), or it may suggest variability in preferred theta frequency according to recording location or even by individual based upon different tuning properties of pyramidal cells and interneurons responsible for theta generation (Canolty and Knight 2010). The exact nature of differences in location, duration, and functional role of slow-theta versus faster oscillatory activity has yet to be fully characterized. For instance, human hippocampal theta may exist on a continuum, modulated by the difficulty of the memory task in which an individual is engaged. Taken together, our results for hippocampal PAC during episodic memory further point to the slow-theta oscillation as a functionally distinct hippocampal frequency band responsible for carrying information related to memory and spatial navigation (Cornwell et al. 2008; Watrous, Lee et al. 2013; Chen et al. 2013). Slow-theta may be the best candidate for a putative correlate of rodent hippocampal theta (Watrous, Lee et al. 2013).

Our results indicate that a PAC analysis of iEEG activity may assist in the identification of brain locations that exhibit long-term potentiation during successful episodic item encoding. We found that the electrodes that exhibit PAC+ effects demonstrate a phase preference near the trough of the slow-theta oscillation for PAC in the hippocampus. Increased gamma activity at this point in the cycle is most propitious for eliciting LTP and contributing to the formation of novel synaptic connections that may be necessary for item encoding (Fries 2005, 2009). In the cortex, for both PAC+ and PAC– electrodes, the preferred phase for the dominant 4–9 Hz oscillation was also near 180° (see Fig. 3). This finding supports the differential importance of slow-theta oscillations in the hippocampus, and supports the possibility of multiply-nested oscillations organized at their base by the hippocampal slow-theta oscillation. The hippocampal PAC– electrodes exhibited theta–gamma coupling at phases more likely to induce long-term depression in synaptic association; however, it is intriguing that the phase difference between the preferred phase for “cortical” slow-theta oscillations and these hippocampal PAC– electrodes (~170°) is similar to the phase offset we previously described for oscillatory synchrony at slow-theta frequencies between the hippocampus and temporal cortex (Wilson et al. 1990; Lega et al. 2011). This finding may support a hypothesis for different amplitude–amplitude or phase–amplitude cross frequency coupling between PAC+ versus – electrodes and cortical electrodes that exhibit PAC in the 4–9 Hz frequency range (see Fig. 4). Non-invasive studies have also recently identified differences in the phase properties of hippocampal PAC for item–context associations (Staudigl and Hanslmayr 2013). Heterogeneity within the hippocampus for a gamma band effect has been observed in animal data (Montgomery and Buzsáki 2007), and for an SME in our own previous data (Lega et al. 2011). Further, we observed effects for PAC in the hippocampus that extend into the beta frequency range for slow-theta coupling. The significance of beta oscillations for episodic memory has garnered recent interest based upon non-invasive human data (Hanslmayr and Staudigl 2014). This remains an area of further investigation, as our own analyses have identified significant beta oscillatory activity in the hippocampus alongside gamma and slow-theta activity (Lega et al. 2011).

We uncovered evidence of a difference between modulation of high and low gamma oscillations by theta phase. The hippocampal-neocortical difference in slow theta versus 4–9 Hz theta for the strongest phase-providing frequency was not identifiable for high gamma oscillations. This may reflect differences in the contribution of local neuronal activity to high versus low gamma oscillatory amplitude, that is, low gamma represents a genuine oscillation rather than aggregated local spiking activity (Manning et al. 2009; Miller et al. 2009; Ray and Maunsell 2011; Crone et al. 2011). Gamma band changes during item encoding (the gamma SME) did not appear to confound our quantification of PAC via the modulation index, as gamma SME effects showed no relationship to PAC magnitude. In contrast, the positive correlation between PAC and the slow-theta band SME fit with an overall picture of select hippocampal sites that exhibit increased slow-theta activity during successful encoding while more nonspecific power and PAC changes occur at adjacent brain sites. This bimodal pattern is consistent with a model in which the hippocampus breaks away from global slow activity, leading to a general decrease in

oscillatory power across the entire formation (Sederberg et al. 2007), but a subset of critical locations exhibit increased theta power which more effectively entrains gamma oscillations (Lega et al. 2011). The fact that this power increase and entrainment occur preferentially at the trough of the theta oscillation, while other sites exhibit coupling at phases less propitious for LTP, lends support to the conclusion that the hippocampal locations picked out by the SME/PAC analysis are the best targets for modulation of memory performance even if the hippocampus as a whole exhibits a mixed pattern of both PAC and SME changes. These findings should assist investigations of entorhinal-hippocampal communication during item retrieval. A sharper focus on the most relevant frequencies may help identify data in support of theories that postulate theta phase differences during this process (Hasselmo and Eichenbaum 2005).

### Supplementary Material

Supplementary material can be found at: <http://www.cercor.oxfordjournals.org/>

### Funding

This work was supported by National Institutes of Health grants MH055687. We are indebted to all patients who have selflessly volunteered their time to participate in our study.

### Notes

*Conflict of Interest:* None declared.

### References

- Addison P. 2002. The illustrated wavelet transform handbook: introductory theory and applications in science, engineering, medicine and finance. Bristol: Institute of Physics Publishing.
- Axmacher N, Henseler M, Jensen O, Weinreich I, Elger C, Fell J. 2010. Cross-frequency coupling supports multi-item working memory in the human hippocampus. *Proc Natl Acad Sci USA*. 107(7):3228–3233.
- Burke J, Zaghoul K, Jacobs J, Williams RB, Sperling MR, Sharan AD, Kahana MJ. 2013. Synchronous and asynchronous theta and gamma activity during episodic memory formation. *J Neurosci*. 33(1):292–304.
- Buzsáki G. 2005. Theta rhythm of navigation: link between path integration and landmark navigation, episodic and semantic memory. *Hippocampus*. 15(7):827–840.
- Canolty RT, Edwards E, Dalal SS, Soltani M, Nagarajan SS, Kirsch HE, Berger MS, Barbaro NM, Knight RT. 2006. High gamma power is phase-locked to theta oscillations in human neocortex. *Science*. 313(5793):1626–1628.
- Canolty RT, Knight RT. 2010. The functional role of cross-frequency coupling. *Trends Cogn Sci*. 14(11):506–515.
- Chen G, King JA, Burgess N, O'Keefe J. 2013. How vision and movement combine in the hippocampal place code. *Proc Natl Acad Sci USA*. 110(1):378–383.
- Chrobak JJ, Buzsáki G. 1998. Gamma oscillations in the entorhinal cortex of the freely behaving rat. *J Neurosci*. 18(1):388–398.
- Clemens Z, Weiss B, Szűcs A, Erőss L, Rásonyi G, Halász P. 2009. Phase coupling between rhythmic slow activity and gamma characterizes mesiotemporal rapid-eye-movement sleep in humans. *Neuroscience*. 163(1):388–396.
- Cohen M, Elger C, Fell J. 2009. Oscillatory activity and phase-amplitude coupling in the human medial frontal cortex during decision making. *J Cogn Neurosci*. 21(2):390–402.
- Cornwell B, Johnson L, Holroyd T, Carver F, Grillon C. 2008. Human hippocampal and parahippocampal theta during goal-directed spatial navigation predicts performance on a virtual Morris water maze. *J Neurosci*. 28(23):5983–5990.
- Crone NE, Korzeniewska A, Franaszczuk P. 2011. Cortical gamma responses: searching high and low. *Int J Psychophysiol*. 79(1):9–15.
- Douchamps V, Jeewajee A, Blundell P, Burgess N, Lever C. 2013. Evidence for encoding versus retrieval scheduling in the hippocampus by theta phase and acetylcholine. *J Neurosci*. 33(20):8689–8704.
- Fell J, Ludowig E, Staesina B, Wagner T, Kranz T, Elger CE, Axmacher N. 2011. Medial temporal theta/alpha power enhancement precedes successful memory encoding: evidence based on intracranial EEG. *J Neurosci*. 31(14):5392–5397.
- Fisher NI. 1993. Statistical analysis of circular data. Cambridge, England: Cambridge University Press.
- Fries P. 2005. A mechanism for cognitive dynamics: neuronal communication through neuronal coherence. *Trends Cogn Sci*. 9(10):474–480.
- Fries P. 2009. Neuronal gamma-band synchronization as a fundamental process in cortical computation. *Annu Rev Neurosci*. 32(1):209–224.
- Hanslmayr S, Staudigl T. 2014. How brain oscillations form memories—a processing based perspective on oscillatory subsequent memory effects. *Neuroimage*. 85:648–655.
- Hasselmo M, Eichenbaum H. 2005. Hippocampal mechanisms for the context-dependent retrieval of episodes. *Neural Netw*. 18(9):1172–1190.
- Jacobs J. 2014. Hippocampal theta oscillations are slower in humans than in rodents: implications for models of spatial navigation and memory. *Philos Trans R Soc Lond B Biol Sci*. 369(1635):20130304.
- Johnson A, Redish A. 2007. Neural ensembles in ca3 transiently encode paths forward of the animal at a decision point. *J Neurosci*. 27(45):12176–12189.
- Lega B, Jacobs J, Kahana M. 2011. Human hippocampal theta oscillations and the formation of episodic memories. *Hippocampus*. 22(4):748–761.
- Manning JR, Jacobs J, Fried I, Kahana MJ. 2009. Broadband shifts in LFP power spectra are correlated with single-neuron spiking in humans. *J Neurosci*. 29(43):13613–13620.
- Maris E, van Vugt MK, Kahana MJ. 2011. Spatially distributed patterns of oscillatory coupling between high-frequency amplitudes and low-frequency phases in human IEEG. *Neuroimage*. 54(2):836–850.
- Miller JF, Kahana MJ, Weidemann CT. 2012. Recall termination in free recall. *Mem Cognit*. 40(4):540–550.
- Miller KJ, Sorensen LB, Ojemann JG, den Nijs M, Sporns O. 2009. Power-law scaling in the brain surface electric potential. *PLoS Comput Biol*. 5(12):e1000609.
- Montgomery SM, Buzsáki G. 2007. Gamma oscillations dynamically couple hippocampal CA3 and CA1 regions during memory task performance. *Proc Natl Acad Sci USA*. 104(36):14495–14500.
- O'Keefe J, Recce ML. 1993. Phase relationship between hippocampal place units and the EEG theta rhythm. *Hippocampus*. 3:317–330.
- Olson I, Moore K, Stark M, Chatterjee A. 2006. Visual working memory is impaired when the medial temporal lobe is damaged. *J Cogn Neurosci*. 18(7):1087–1097.
- Paller KA, Wagner AD. 2002. Observing the transformation of experience into memory. *Trends Cogn Sci*. 6(2):93–102.
- Penny W, Duzel E, Miller K, Ojemann J. 2008. Testing for nested oscillation. *J Neurosci Methods*. 174(1):50–61.
- Ray S, Maunsell J. 2011. Different origins of gamma rhythm and high-gamma activity in macaque visual cortex. *PLoS Biol*. 9(4):e1000610.
- Rutishauser U, Ross I, Mamelak A, Schuman E. 2010. Human memory strength is predicted by theta-frequency phase-locking of single neurons. *Nature*. 464(7290):903–907.
- Sederberg PB, Kahana MJ, Howard MW, Donner EJ, Madsen JR. 2003. Theta and gamma oscillations during encoding predict subsequent recall. *J Neurosci*. 23(34):10809–10814.
- Sederberg PB, Schulze-Bonhage A, Madsen JR, Bromfield EB, McCarthy DC, Brandt A, Tully MS, Kahana MJ. 2007. Hippocampal and neocortical gamma oscillations predict memory formation in humans. *Cereb Cortex*. 17(5):1190–1196.
- Shirvalkar PR, Rapp PR, Shapiro ML. 2010. Bidirectional changes to hippocampal theta-gamma comodulation predict memory for recent spatial episodes. *Proc Natl Acad Sci USA*. 107(15):7054–7059.

- Staudigl T, Hanslmayr S. 2013. Theta oscillations at encoding mediate the context-dependent nature of human episodic memory. *Curr Biol*. 23(12):1101–1106.
- Steinvorth S, Wang C, Ulbert I, Schomer D, Halgren E. 2009. Human entorhinal gamma and theta oscillations selective for remote autobiographical memory. *Hippocampus*. 20(1):166–173.
- Tort A, Komorowski R, Manns J, Kopell N, Eichenbaum H. 2009. Theta–gamma coupling increases during the learning of item–context associations. *Proc Natl Acad Sci USA*. 106(49):20942–20947.
- Tort A, Kramer M, Thorn C, Gibson D, Kubota Y, Graybiel A, Kopell N. 2008. Dynamic cross-frequency couplings of local field potential oscillations in rat striatum and hippocampus during performance of a T-maze task. *Proc Natl Acad Sci USA*. 105(51):20517–20522.
- Tort A, Rotstein H, Dugladze T, Gloveli T, Kopell N. 2007. On the formation of gamma-coherent cell assemblies by oriens lacunosum-moleculare interneurons in the hippocampus. *Proc Natl Acad Sci USA*. 104(33):13490–13495.
- Tort AB, Komorowski R, Eichenbaum H, Kopell N. 2010. Measuring phase-amplitude coupling between neuronal oscillations of different frequencies. *J Neurophysiol*. 104(2):1195–1210.
- Tulving E. 1983. *Elements of episodic memory*. Oxford: Oxford University Press.
- van der Meij R, Kahana MJ, Maris E. 2012. Phase-amplitude coupling in human ECoG is spatially distributed and phase diverse. *J Neurosci*. 32(1):111–123.
- Vinck M, Lima B, Womelsdorf T, Oostenveld R, Singer W, Neuenschwander S, Fries P. 2010. Gamma phase shifting in awake monkey visual cortex. *J Neurosci*. 30(4):1250–1257.
- Voytek B, Canolty R, Shestyuk A, Crone N, Parvizi J, Knight R. 2010. Shifts in gamma phase–amplitude coupling frequency from theta to alpha over posterior cortex during visual tasks. *Front Hum Neurosci*. 4(191):1–8.
- Watrous AJ, Lee DJ, Izadi A, Gurkoff GG, Shahlaie K, Ekstrom AD. 2013. A comparative study of human and rat hippocampal low-frequency oscillations during spatial navigation. *Hippocampus*. 23(8):656–661.
- Watrous AJ, Tandon N, Conner CR, Pieters T, Ekstrom AD. 2013. Frequency-specific network connectivity increases underlie accurate spatiotemporal memory retrieval. *Nat Neurosci*. 16(3):349–356.
- Wilson C, Isokawa M, Babb T, Crandall P. 1990. Functional connections in the human temporal lobe. *Exp Brain Res*. 82(2):279–292.
- Wulff P, Ponomarenko A, Bartos M, Korotkova T, Fuchs E, Böhner F, Both M, Tort A, Kopell N, Wisden W et al. 2009. Hippocampal theta rhythm and its coupling with gamma oscillations require fast inhibition onto parvalbumin-positive interneurons. *Proc Natl Acad Sci USA*. 106(9):3561–3566.